CROSS-SECTION RATIO OF THE CHARMONIA STATES $\psi(2S)$ AND $J/\psi(1S)$ IN EXCLUSIVE PHOTOPRODUCTION AT HERA*

Grzegorz Grzelak

on behalf of the ZEUS Collaboration

University of Warsaw, Poland

Received 30 November 2022, accepted 12 December 2022, published online 25 May 2023

The exclusive photoproduction reactions $\gamma^* p \to J/\psi(1S)p$ and $\gamma^* p \to \psi(2S)p$ have been measured with the ZEUS detector at the HERA collider. The used data sample corresponds to an integrated luminosity of 373 pb^{-1} collected during the HERA-II running period. The analysis was performed in the kinematic range of $30 < W < 180$ GeV, $Q^2 < 1$ GeV^2, and $|t| < 1$ GeV^2, where W is the photon–proton centre-of-mass energy, Q^2 is the virtuality of the photon (γ^*), and t is the squared four-momentum transfer at the proton vertex. The following decay channels were investigated: $J/\psi(1S) \to \mu^+\mu^-$, $\psi(2S) \to \mu^+\mu^-$, and $\psi(2S) \to J/\psi(1S)\pi^+\pi^-$ with subsequent decay $J/\psi(1S) \to \mu^+\mu^-$.

DOI:10.5506/APhysPolBSupp.16.5-A32

1. Exclusive heavy vector-meson production in *ep* collisions

Exclusive electroproduction and photoproduction of charmonia states $J/\psi(1S)$ and $\psi(2S)$ have been widely studied at HERA [1–4]. These processes can be described by models based on perturbative QCD (pQCD) making use of the hard scale provided by the large mass of the charm quark.

The process is assumed to factorize in three subsequent steps as presented in Fig. 1: first, the photon fluctuates into a $c\bar{c}$ pair of small transverse size and lifetime long compared to the time of interaction. Subsequently, it interacts with the proton via the exchange of gluons in a colour-singlet state, and finally, forms a heavy vector meson (VM) which inherits the quantum numbers of the initial photon. The cross section for this process is therefore sensitive to the gluon density in the proton.

* Presented at the Diffraction and Low-x 2022 Workshop, Corigliano Calabro, Italy, 24–30 September, 2022.

The $\psi(2S)$ and $J/\psi(1S)$ mesons have the identical composition of valence quarks but different distributions of the radial wave functions. As their mass difference is small compared to the HERA centre-of-mass energy, the kinematical threshold effects can be neglected and the measurement allows for QCD predictions of the wave function dependence of the $c\bar{c}$–proton cross section to be tested. A dumping of the $\psi(2S)$ production rate with respect to the $J/\psi(1S)$ is expected, as the $\psi(2S)$ wave function has a radial node at $r \sim 0.4$ fm close to the specific distance of the virtual $c\bar{c}$ quarks.

A significant source of background comes from the diffractive reaction (Fig. 1, right) $ep \to \mathrm{VM} + e + Y$, where the proton dissociates into a multi-hadronic state Y, which is described by M_Y, the invariant mass of the diffractively produced system Y.

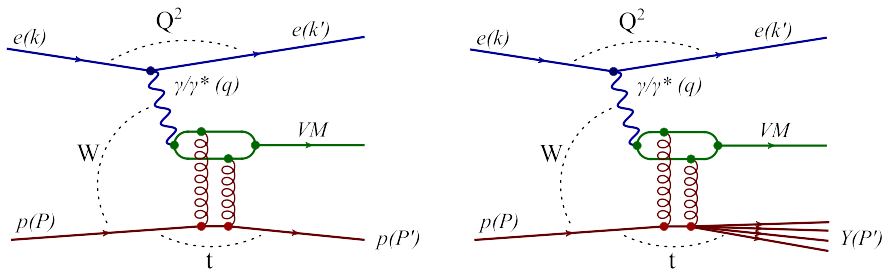

Fig. 1. Lowest order diagrams with two gluons exchanged for the exclusive and photon-dissociative vector-meson photoproduction in ep interaction.

2. Experimental results

Exclusive $\psi(2S)$ and $J/\psi(1S)$ events were selected using dedicated triggers and software criteria. For 2- and 4-prong decay channels, the selection was driven by muons by requiring a pair of oppositely charged tracks in the central tracker originating from the primary vertex and matched to the central calorimeter muon signal (MIP). At least one such a track starting from the trigger level should be also associated with a muon chambers deposit or with a hit pattern in the backing calorimeter consistent with a muon. No other activity (except for the slow pions signal for the 4-prong channel) should be observed in the detector. More details of the analysis can be found in the publication in preparation [5].

Figure 2 presents an example of the di-muon invariant mass distribution obtained for the full phase space of this analysis. Monte Carlo (MC) distributions for simulated events are also shown for the exclusive production of $J/\psi(1S)$ and $\psi(2S)$ (Diffvm [6]) and for a continuous background of muon pairs (Grape [7]) from the Bethe–Heitler (BH) process. The relative contribution of the various MC processes was determined from the fractional fit to the

2-prong mass distribution. Figure 3 contains the invariant mass distribution $M(\mu^+\mu^-\pi^+\pi^-)$ (left) and the mass difference $M(\mu^+\mu^-\pi^+\pi^-) - M(\mu^+\mu^-)$ (right) for the 4-prong decay of $\psi(2S)$. The relative fraction of elastic and proton-dissociative processes was determined from a fit to the $|t|$ distribution. The advantage of including the 4-prong channel, despite its much lower efficiency, is the high purity of this almost background-free final state.

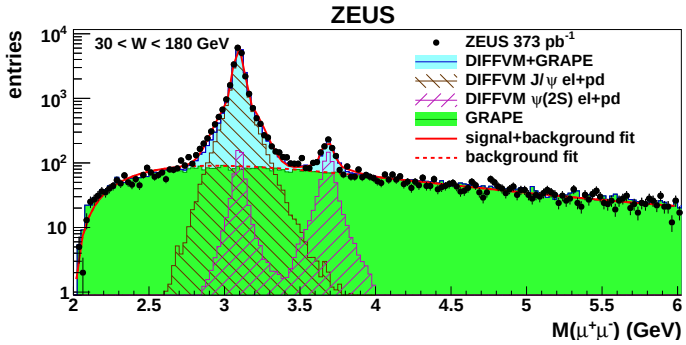

Fig. 2. Invariant mass distribution $M(\mu^+\mu^-)$ of di-muon pairs (solid circles) with error bars denoting statistical uncertainties [5]. Monte Carlo distributions for various simulated processes are also shown (see the legend and Section 2).

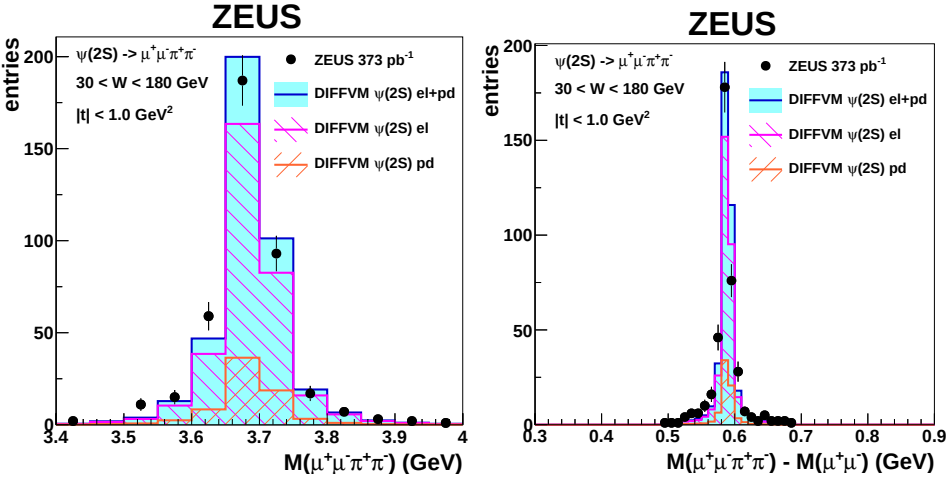

Fig. 3. Invariant mass distribution, $M(\mu^+\mu^-\pi^+\pi^-)$ (left), and difference in invariant masses, $M(\mu^+\mu^-\pi^+\pi^-) - M(\mu^+\mu^-)$ (right) for the 4-prong decay of $\psi(2S)$ in photoproduction events (solid circles) [5]. Monte Carlo distributions for simulated events are also shown (see the legend and Section 2).

The cross-section ratio $R = \sigma_{\psi(2S)}/\sigma_{J/\psi(1S)}$ measured in the 2- and 4-prong channels provided consistent results which were combined as the weighted mean value. In the full phase space of this analysis, it is

$$R = 0.146 \pm 0.010\,(\text{stat.})\,^{+0.016}_{-0.020}\,(\text{syst.})\,,$$

where the first uncertainty is statistical and the second is the sum of all systematic uncertainties added in quadrature.

In Fig. 4, the cross-section ratios differential in W and $|t|$ are shown. As a function of W, the value of R is consistent with a constant value. A moderate rise of R with increasing $|t|$ is visible. The data presented in Fig. 4, left are compatible with previous results from H1 [3, 4]. The value of R given above is also plotted in Fig. 5 and compared with other data from photoproduction and deep inelastic scattering (DIS) as a function of Q^2. The value measured in this analysis confirms the previous measurements in photoproduction [3, 4].

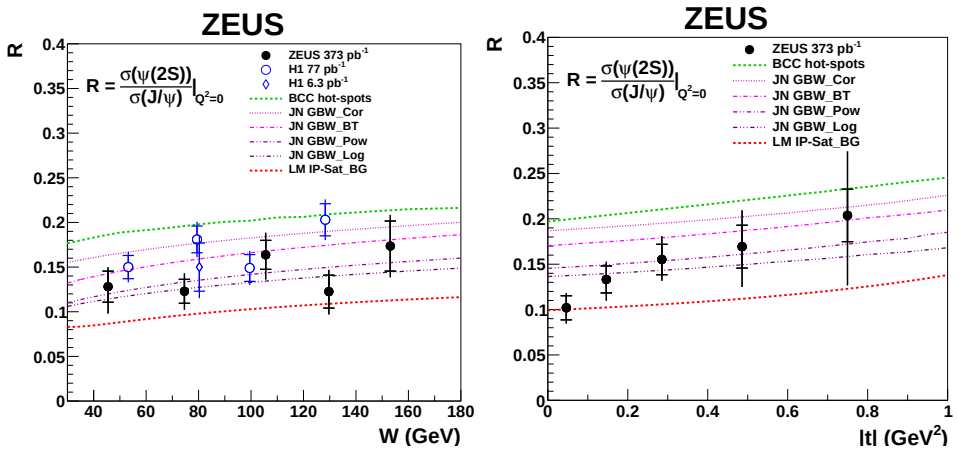

Fig. 4. Cross-section ratio $R = \sigma_{\psi(2S)}/\sigma_{J/\psi(1S)}$ in photoproduction as a function of W (left) and $|t|$ (right) [5]. The ZEUS measurements are shown as solid circles. In the left plot the previous measurements from H1 (open points) [3, 4] are also presented. Various QCD-inspired models are compared to the data and shown as lines [8–17] (see the legend and Section 3).

3. Comparison with theoretical models

In Figs. 4 and 5, predictions from theoretical models are compared to photoproduction and DIS data as a function of W, $|t|$, and Q^2.

The hot-spots model from Bendová, Čepila, and Contreras (BCC) [8] is related to energy-dependent areas of high gluon density in the proton.

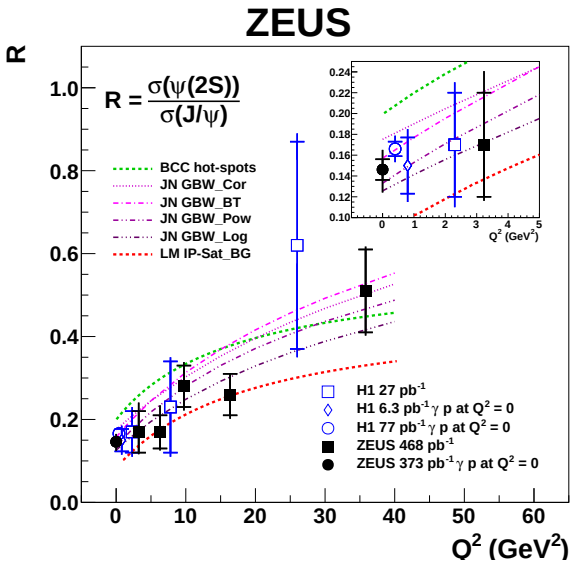

Fig. 5. Cross-section ratio $R = \sigma_{\psi(2S)}/\sigma_{J/\psi(1S)}$ as a function of Q^2. The measurement from this analysis of photoproduction data is shown at $Q^2 = 0$ GeV^2 (solid circle) [5]. Previous data in photoproduction from H1 are also presented (open circle and diamond) [3, 4], and data from deep inelastic scattering from H1 (open squares) [2] and ZEUS (solid squares) [1]. Various QCD-inspired models are compared to the data and shown as lines [8–17] (see the legend and Section 3).

The model from Nemchik *et al.* [9–11] (JN) delivers predictions with various schemes of colour-dipole interactions and quarkonia potentials used for the determination of wave functions. The predictions shown are based on the Golec-Biernat–Wüsthoff (GBW) colour-dipole model [12, 13]. The included quarkonia potentials were: the so-called Buchmüller–Tye (BT), logarithmic (Log), Cornell (Cor), and power-law (Pow).

Lappi and Mäntysaari [14] (LM) utilize the BFKL evolution and the IP-Sat model [15] to describe vector-meson production in ep collisions in the dipole picture. The wave functions of the $J/\psi(1S)$ and $\psi(2S)$ have been calculated using the boosted Gaussian (BG) prescription [16, 17].

All models predict a slow increase in R as a function of W. The predicted slopes are very similar for all models but the absolute values of the intercept differ by up to a factor of two. All models also predict an increase in R with increasing $|t|$, and again provide similar gradients but different absolute values. Taking into account the experimental uncertainties in the data and the spread of the models, the description of the data is good.

In Fig. 5, model predictions are compared to photoproduction and DIS data as a function of Q^2. All models predict a strong increase in R with increasing Q^2, which is in agreement with the tendency observed in the data. The most precise photoproduction points have the potential to constrain the models further.

Overall, the predictions from the three models, BCC, JN, and LM, give a good description of the W, $|t|$, and Q^2 dependence of the ratio R.

We would like to express our special thanks to Dagmar Bendová, Jan Čepila, Michal Křelina, Jan Nemchik, and Heikki Mäntysaari for providing model predictions and for fruitful discussions.

REFERENCES

[1] ZEUS Collaboration (H. Abramowicz *et al.*), *Nucl. Phys. B* **909**, 934 (2016).
[2] H1 Collaboration (C. Adloff *et al.*), *Eur. Phys. J. C* **10**, 373 (1999).
[3] H1 Collaboration (C. Adloff *et al.*), *Phys. Lett. B* **541**, 251 (2002).
[4] H1 Collaboration (C. Adloff *et al.*), *Phys. Lett. B* **421**, 385 (1998).
[5] ZEUS Collaboration (I. Abt *et al.*), *J. High Energ. Phys.* **2022**, 164 (2022), arXiv:2206.13343 [hep-ex].
[6] B. List, A. Mastroberardino, in: A.T. Doyle, G. Grindhammer, G. Ingelman, H. Jung (Eds.) «Proceedings of the Workshop on Monte Carlo Generators for HERA Physics», *DESY*, Hamburg, Germany 1999, p. 396.
[7] T. Abe, *Comput. Phys. Commun.* **136**, 126 (2001).
[8] D. Bendová, J. Čepila, J.G. Contreras, *Phys. Rev. D* **99**, 034025 (2019).
[9] M. Křelina *et al.*, *Eur. Phys. J. C* **79**, 154 (2019).
[10] J. Čepila *et al.*, *Eur. Phys. J. C* **79**, 495 (2019).
[11] B.Z. Kopeliovich, M. Křelina, J. Nemchik, *Phys. Rev. D* **103**, 094027 (2021).
[12] K.J. Golec-Biernat, M. Wüsthoff, *Phys. Rev. D* **59**, 014017 (1998).
[13] K.J. Golec-Biernat, M. Wüsthoff, *Phys. Rev. D* **60**, 114023 (1999).
[14] T. Lappi, H. Mäntysaari, *Phys. Rev. C* **83**, 065202 (2011).
[15] A.H. Reazeian *et al.*, *Phys. Rev. D* **87**, 034002 (2013).
[16] T. Lappi, H. Mäntysaari, *PoS* **(DIS2014)**, 069 (2014).
[17] H. Kowalski, L. Motyka, G. Watt, *Phys. Rev. D* **74**, 074016 (2006).